Journal of Neurodevelopmental Cognition

Journal of Neurodevelopmental Cognition 6(1) (2025) 18- 32 10.48308/jncog.2025.238626.1012

ISSN: 2645-565X

http://www.jncog.sbu.ac.ir

Enhancement of Signal Transmission by Delay Selection in Feedforward Networks Through Spike Timing-Dependent Synaptic Plasticity

Ali Ghadiri[1], Hedyeh Rezaei [2], and Alireza Valizadeh [1*]

[1] *Institute for Advanced Studies in Basic Sciences (IASBS), Zanjan, Iran*

[2] *University Medical Center Hamburg-Eppendorf (UKE), Hamburg, Germany*

Abstract

Spike timing-dependent plasticity (STDP) is a fundamental mechanism that modulates synaptic strength in response to the precise temporal relationships between input and output spikes. However, the exact role of transmission delays in this mechanism, particularly at the network level, remains unclear. Delays introduce an additional layer of complexity, as they directly influence the timing of spikes and consequently the direction and magnitude of synaptic modifications through STDP. Understanding how these delays shape and are shaped through plasticity rules is critical to reveal their role in neural computations. In this study, we explored the effects of repetitive presentations of synchronous spike volleys on the distribution of transmission delays in a feedforward (FF) network through STDP. Our findings showed that STDP preferentially selected connections with shorter transmission delays, whereas connections with longer delays were weakened and pruned from the network. We showed that "learning of delays" by the impact of synchronous pulse packets propagated forward; that is, the modification of the delays began from the connections between upstream layers and continued to downstream ones. This forward propagation of the delay selection process was accompanied by the successful transmission of synchronous signals along the network. The interaction between transmission delays and synaptic modification established a dynamic feedback loop. The transmission of synchronous signals drove the selective strengthening or weakening of connections, while the evolving synaptic structure, in turn, shaped the pathways for signal propagation. This bidirectional interplay highlighted the fundamental role of delays in orchestrating both network dynamics and the plasticity rule.

Keywords*:* Spike timing-dependent plasticity rule, delay selection, feedforward networks, signal transmission.

* Corresponding author

Email addresses: valizadeh@gmail.com

Received: February 2025 Accept: March 2025

1. Introduction

Activity-dependent synaptic modification is shaped by the precise timing of spikes from both pre- and postsynaptic neurons. Studies have shown that an excitatory synapse targeting an excitatory neuron is strengthened when a presynaptic spike precedes a postsynaptic spike. In contrast, if the postsynaptic spike occurs before the presynaptic spike, the synapse weakens (Caporale & Dan, 2008; Do, 1949; Markram et al., 1997).

Experimental and computational studies have demonstrated that early input spikes are particularly effective in driving postsynaptic neurons. When such inputs are repeatedly presented in the same spike pattern, they enhance synaptic strength and reduce the latency of the postsynaptic response (Song et al., 2000; Gerstner & Kistler, 2002; Guyonneau et al., 2005; VanRullen & Thorpe, 2001). This temporal sensitivity underscores the importance of spike timing in sculpting neural responses and optimizing information transfer.

Synchronization of spikes among a subgroup of neurons is crucial for effectively driving cortical networks, particularly in response to sparse thalamic input (Wang et al., 2010). Such synchronization can propagate through the layers of a feedforward (FF) network while preserving temporal precision (Kumar et al., 2008; Kumar et al., 2010). However, successful propagation requires sufficiently strong stimuli which can trigger spike volleys with a high spike count and minimal timing dispersion. Variations in transmission delay can disrupt this synchronization by further dispersing incoming spikes. These delays are influenced by factors such as the physical distance between cortical regions and conduction velocities, both of which can vary significantly across brain areas (Kress et al., 2008; Kusano, 1966; Pérez et al., 2011).

Transmission delays not only shape synaptic efficacy but also play a critical role in defining information and signal transmission within neural circuits (Pariz et al., 2021; Rezaei et al., 2020). Delays influence the synchronization of neuronal populations, affecting the generation and maintenance of oscillatory rhythms (Roohi & Valizadeh, 2022; Sadeghi & Valizadeh, 2014; Ghasemi Esfahani & Valizadeh, 2014) that underlie cognitive functions such as perception, attention, and working memory. In functional networks, delays modulate phase relationships between neuronal groups, thereby affecting the coherence of neural oscillations across different frequency bands (Ziaeemehr & Valizadeh, 2021; Ziaeemehr et al., 2020). This temporal structuring is crucial for coordinating activity across distant brain regions, enabling efficient communication and integration of information. Moreover, variations in conduction delays contribute to the formation of dynamic network states, where oscillatory interactions can either facilitate or suppress information flow depending on their phase alignment (Esfahani et al., 2016). These findings suggest that delays are not merely constraints but fundamental parameters that actively shape the functional architecture of the brain.

Moreover, transmission delays, critically determine the emergent structure of neuronal networks through STDP. By biasing synaptic modifications based on the precise timing of pre- and postsynaptic spikes, delays actively contribute to the formation of stable connectivity patterns that underlie efficient information transfer and robust network dynamics (Madadi Asl et al., 2018; Madadi Asl et al., 2023). Interestingly, one study suggested that during the propagation of synchronous activity through layers, as well as during repeated presentations of spike volleys, transmission delays in the FF direction influence synaptic conductance. Shorter

delays are associated with stronger conductance compared to longer delays (Suri & Sejnowski, 2002). This highlights the role of transmission delay as not merely a passive factor but an active determinant in shaping synaptic dynamics and network efficiency.

2. Method

Simulations were performed using the NEST simulator (v2.16.0) in Python, employing a temporal resolution of 0.1 ms to ensure precise representation of neuronal dynamics (Gewaltig & Diesmann, 2007; Morrison et al., 2007). Neurons were implemented via a leaky integrate-and-fire framework augmented with conductance-based synaptic interactions. The governing dynamics of the membrane potential adhered to the following equation:

$$C_m \frac{dV_m}{dt} = -G_{leak}(V_m(t) - V_{reset}) + I_{syn}(t) \quad (1)$$

where C_m is the membrane capacitance, G_{leak} the leak conductance, V_{reset} the reset potential, and $I_{syn}(t)$ the total synaptic current. Neurons fired when V_m reached a threshold value, resetting to V_{reset} and entering a refractory period (2 ms). Model parameters are detailed in *Table 1*. Initial membrane potentials were uniformly randomized to mitigate artificial synchrony.

Synaptic currents were derived from time-varying conductances described as:

$$I_{syn}(t) = G_{syn}(t)(V_m(t) - E_{syn}) \quad (2)$$

The dynamics of $G_{syn}(t)$ for each presynaptic spike followed an exponential decay:

$$G_{syn}(t) = G_{syn} \exp\left(\frac{-(t - t_s)}{\tau_{syn}}\right) \quad (3)$$

Where t_s is the spike time, τ_{syn} the synaptic time constant, and E_{syn} the synaptic reversal potential. Distinct parameters were used for excitatory and inhibitory synapses to reflect physiological properties (refer to *Table 1*).

Network architecture comprised within-layer random excitatory (E) and inhibitory (I) connections as well as inter-layer excitatory FF pathways. Inter-layer synaptic connections adapted according to a spike timing-dependent plasticity (STDP) mechanism:

$$\Delta w = \begin{cases} -\lambda \alpha e^{-\frac{|\Delta t|}{\tau_-}}, & \Delta t < 0 \\ \lambda e^{-\frac{|\Delta t|}{\tau_+}}, & \Delta t \geq 0 \end{cases} \quad (4)$$

This rule reinforced the temporal correlation between presynaptic and postsynaptic spikes, yielding a bimodal weight distribution between zero and W_{max} (upper limit for synaptic modifications). For more detailed information, refer to *Table 1*.

External inputs were generated through independent Poisson processes with different rates for E and I neurons to simulate asynchronous irregular (AI) background activity. Additionally, pulse packets (spike volleys) stimulation was delivered to designated neurons in the initial layer, with each packet containing 50 spikes temporally dispersed around a central time point by a Gaussian distribution (σ = 2 ms).

To assess the irregularity of spike trains in excitatory neurons, we computed the coefficient of variation of inter-spike intervals (CV_{ISIs}) as follow:

$$\mathrm{CV_{ISIs}} = \frac{\sigma_{ISIs}}{\mu_{ISIs}} \quad (5)$$

To quantify the extent to which spike volleys drove the target neurons in the presence of AI background activity, we calculated the Signal-to-Noise Ratio (SNR) as the ratio of the variance of the spike count vector x(t) (bin = 10 ms) during the stimulus period to that during ongoing background activity:

$$\mathrm{SNR} = \frac{Var[x(t)^{stim}]}{Var[x(t)^{ongoing}]} \quad (6)$$

A critical feature of the model was the inclusion of spike transmission delays, that is the time needed for the propagation of the spike along axons and dendrites. The FF axonal delays in our computational model were initially drawn from a wide distribution, whereas dendritic delays were fix at 0.1 ms. These delays played a pivotal role in shaping the network's temporal dynamics, particularly in the context of STDP-driven plasticity and the propagation of synchronous activity. This mechanism forms the core focus of the current study.

To incorporate biologically plausible transmission delays in NEST, axonal conduction times were modeled explicitly. Intermediate relay neurons were introduced to emulate these delays, replicating presynaptic spiking activity with precise temporal offsets. This design effectively segregated axonal delays from dendritic delays, preserving fidelity in synaptic plasticity while adhering to known transmission dynamics.

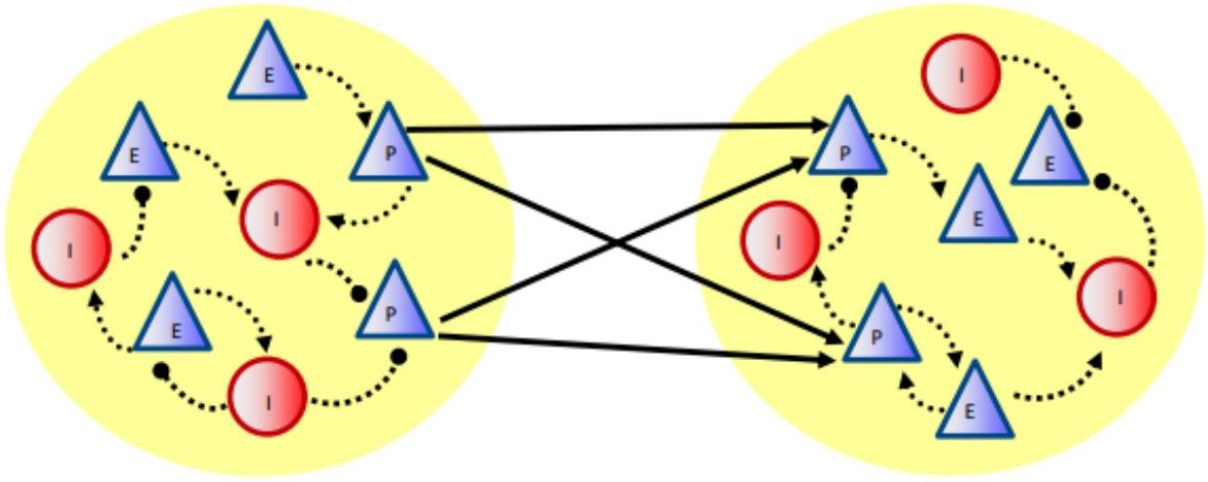

Figure 1: **Schematic representation of a bi-layer network structure.** Excitatory neurons (blue triangles) and inhibitory neurons (red circles) are randomly interconnected within each layer. A subset of excitatory neurons, designated as projection neurons (P neurons), project to a subset of excitatory neurons in the next layer in an all-to-all manner, forming a FF network. The projection sub-population constitutes approximately one-third of the excitatory neurons in each layer network. Within-layer connection weights are fixed according to the parameters listed in Table 1, while inter-layer E-to-E connections evolve based on the STDP rule with parameters presented in Table 1.

Table 1: Summary of Model Parameters

Name	Value	Description
		Neuron model parameters
C_m	250 pF	Membrane capacitance
G_{leak}	16.67 nS	Membrane leak conductance
V_{th}	-54 mV	Firing threshold
V_{reset}	-70 mV	Reset potential
τ_{ref}	2 ms	Refractory time period
		Synapse model parameters
τ_{exc}	3 ms	Decay time constant of excitatory synaptic conductance
τ_{inh}	8 ms	Decay time constant of inhibitory synaptic conductance
E_{syn}^{exc}	0 mV	Reversal potential of excitatory synapses
E_{syn}^{inh}	-80 mV	Reversal potential of inhibitory synapses
J_{ee}	0.33 nS	Within-layer excitatory-to-excitatory synaptic strength
J_{ei}	5.5 nS	Within-layer excitatory-to-inhibitory synaptic strength
J_{ie}	-6.2 nS	Within-layer inhibitory-to-excitatory synaptic strength
J_{ii}	-15.0 nS	Within-layer inhibitory-to-inhibitory synaptic strength
J_{pe}	0.25 nS	Synaptic strength from Poisson spike train to exc pop
J_{pi}	0.4 nS	Synaptic strength from Poisson spike train to inh pop
J_{pp}	0.4 nS	Synaptic strength from pulse packet to P neurons
d_E	1 ms	Within-layer excitatory synaptic delay
d_I	2 ms	Within-layer inhibitory synaptic delay
		STDP Parameters
λ	0.04	Learning rate
α	0.9	Modulates the magnitude of depression increments by $\lambda\alpha$
τ_+	15.9 ms	STDP time constant for potentiation
τ_-	19.3 ms	STDP time constant for depression
		Network model parameters
N_{exc}	200	Number of excitatory neurons per layer
N_{inh}	50	Number of inhibitory neurons per layer
N_{proj}	70	Number of projecting neurons per layer

ε	0.2	Within-layer connection probability
ε_{pp}	1.0	Inter-layer connection probability

3. Results

Evolution of FF synaptic strengths in a bi-layer FF network

To establish the network background state and calibrate the balance of excitatory Poisson inputs to excitatory and inhibitory neuron populations, we systematically varied the Poisson input rate to the network and analyzed the resulting subthreshold activity. Specifically, we adjusted the Poisson input rate to the excitatory population while keeping the input rate to the inhibitory population constant. This approach enabled us to calculate the mean and standard deviation of neurons' membrane potentials for both excitatory and inhibitory neurons, providing a baseline characterization of the background activity of the network (Figure 2, top row of panel (a)). By applying three different Poisson input rates to the excitatory neurons, we induced three corresponding activity levels, as depicted in the two lower rows of Figure 2a. Across all these conditions, excitatory neurons exhibited low firing rates with high variability, quantified by coefficients of variation of inter-spike intervals (CV_{ISIs}) around unity, as shown in Figure 2, bottom row.

Next, we introduced FF excitatory connections between two identical network layers with the same Poisson input rate to excitatory neurons in each layer network. These connections were organized in an all-to-all manner such that every projection neuron in the first layer was connected to all projection neurons in the second layer. The initial synaptic strengths of these FF connections were drawn from a normal distribution with a mean of 0.1 nS and a standard deviation of 0.01 nS. These connections were plastic, governed by a spike timing-dependent plasticity (STDP) rule with parameters λ= 0.04 and W_{max}= 0.4 nS, allowing for dynamic modification of synaptic strengths based on the spike timing. The FF delays were drawn from a wide uniform distribution ranging from 2 to 16 ms.

The Pulse packets were introduced into the projection neurons of the first layer at mean intervals of 250 ms, with fluctuations of ±40 ms around the mean arrival times. The simulation spanned a total of 100 seconds, and was divided into three distinct phases. During the initial 5 seconds no pulse packets were applied, providing a baseline period to observe network activity prior to learning. The pulse packets were then applied for the following 85 seconds, marking the learning phase driven by the STDP rule. Finally, the network response to pulse packets was recorded during the last 10 seconds, representing the post-learning phase.

The results demonstrate that, regardless of the input rate, connections with shorter transmission delays were consistently strengthened, while connections with longer delays were weakened (Figure 2b, c). The primary distinction between the three asynchronous irregular

activity states, each associated with a different firing rate, lies in the number of connections which were either strengthened or pruned. When the increased Poisson input rate to excitatory neurons raised the mean membrane potential of these neurons closer to the firing threshold, a greater number of connections were weakened. Given the initial distribution of delays, longer delays were inherently more likely to be depressed. However, increasing the input rate to excitatory neurons lowered the threshold delay above which connections were eliminated.

A notable outcome of this process was the reduction in the average delay of strengthened connections (defined as the connections with weights greater than $0.8W_{max}$, as shown in Figure 2d), which ultimately led to a faster signal propagation to the second layer. Furthermore, the resulting narrower distribution of delays reduced the temporal disparity of spikes arriving at the second layer, thereby facilitating more efficient and coherent signal transmission.

To further clarify this observation, when the membrane potential of neurons approached the firing threshold, the excitability of postsynaptic neurons increased. This heightened excitability caused postsynaptic neurons to respond preferentially to a smaller subset of incoming spikes within each pulse packet, specifically those spikes which arrived through connections with shorter delays. Additionally, the increased excitability enabled postsynaptic neurons to fire spikes more quickly following each synchronous input.

The earlier spiking of postsynaptic neurons resulted in a larger proportion of presynaptic spikes arriving after the postsynaptic spikes, which, according to the STDP rule, led to the weakening of a greater number of connections. This mechanism underlies the observed pruning of connections with longer delays and the strengthening of connections with shorter delays. Due to the increased weakening of connections in this scenario, the average weight is lower through STDP (Figure 2e).

It is worth noting that when neurons in the second layer were activated in response to inputs transmitted through shorter-delay inter-layer connections, subsequent inputs were less likely to elicit additional responses. This reduced responsiveness is driven by two key mechanisms: First, the refractory period of individual neurons, lasting for 2 milliseconds, temporarily prevented them from firing again. Second, recurrent inhibitory connections within the second layer increased inhibitory activity for a duration corresponding to the network's amplification dynamics as well as the decay time constant of inhibitory connections, which is typically on the order of tens of milliseconds. Together, these mechanisms rendered the network unresponsive to inputs arriving after the initial spikes of the target population. This dynamic effectively reinforced the preference for shorter-delay connections by selectively strengthening the impact of early-arriving inputs.

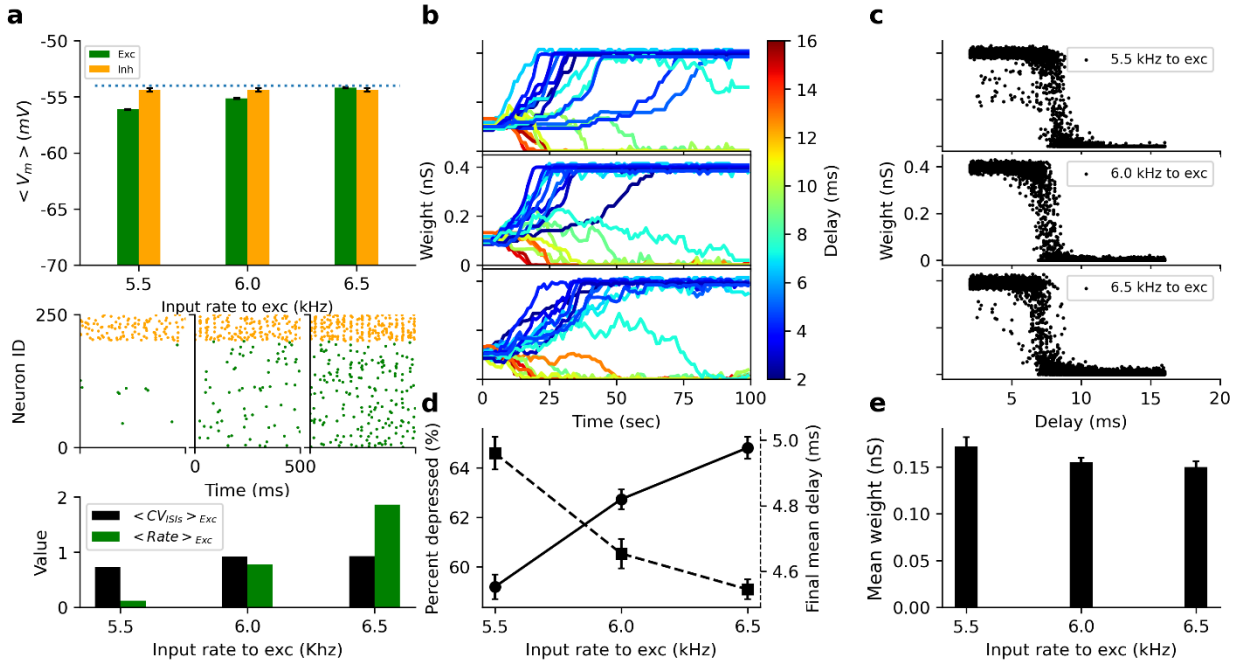

Figure 2: ***Selection of shorter transmission delays in pulse packet propagation.*** ***(a)*** *The mean membrane potential of excitatory (green bars) and inhibitory (orange bars) neurons is shown for three different Poisson input rates to the excitatory neurons' population when the network was isolated. Error bars represent the standard deviation of the membrane potentials. For the three cases, the spiking activity of neurons is displayed as raster plots. Irregularity of excitatory neurons' activity is quantified by coefficient of variation of inter-spike intervals for each excitatory neuron, averaged across all excitatory neurons for each case. Additionally, the mean firing rate of excitatory neurons is shown to be increasing with increased input Poisson rate to excitatory neurons.* ***(b)*** *Weight changes for 20 FF connections are shown under the three background activity conditions (top: 5.5 kHz to exc, middle: 6.0 kHz to exc, bottom: 6.5 kHz to exc). The color of each plot represents the spike transmission delay of the corresponding connection.* ***(c)*** *The results indicate that connections with shorter transmission delays were strengthened, while longer delays tended to be weakened. This trend is clearly illustrated in the final distribution of weights and transmission delays in each initial condition.* ***(d)*** *The number of weakened connections is higher when background fluctuations are closer to the spike threshold. The weakening of a larger number of connections with longer delays results in a reduction of the mean transmission delay for strengthened connections. Ultimately, these changes lead to faster responses in the receiving layer.* ***(e)*** *The mean final weight of connections (during the post-learning phase) is lower when the mean membrane potential of neurons is closer to the threshold.*

As an illustrative example, we set the input rate to excitatory neurons to 6.5 kHz to bring their background activity close enough to the firing threshold, and investigated the possibility of propagation of pulse packets across the FF network. As also suggested by the Signal-to-Noise ratio (SNR) before and after learning in Figure 3, the propagation of pulse packets increased significantly after the learning phase.

The net result of this process is that connections with shorter transmission delays were strengthened, whereas those with longer delays were weakened. Consequently, signals arrive at the second layer both more quickly and in a more synchronized manner, as the reduced temporal dispersion of inputs fostered faster and more reliable propagation of pulse packets.

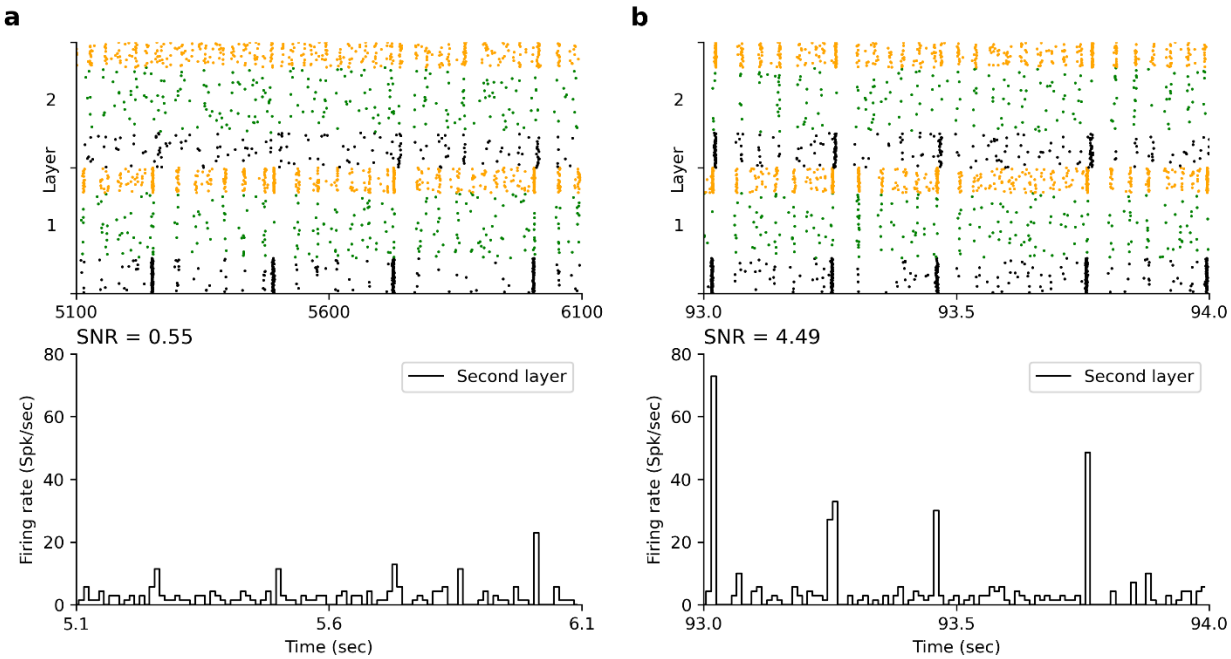

Figure 3: ***Enhancement of pulse packet propagation through STDP****. Pulse packet propagation was significantly enhanced after the learning process* ***(b)*** *due to pruning of connections with larger transmission delays compared to pre-learning phase* ***(a)****. In the top rows, the spiking activity of the projection neurons (black), excitatory neurons (green), and inhibitory neurons (orange) are shown. In the bottom rows, the rate histogram of the projection neurons in the second layer is displayed (bin = 10 ms). The SNR increased after the modification of synaptic connections through STDP.*

Facilitation of pulse packet propagation in a multi-layer network through forward-propagation of synaptic modifications

To investigate how the results of the two-layer network motif translate to a FF network, we considered the modification of synapses and its effect on the transmission of pulse packets across a multi-layer FF network with distributed inter-layer transmission delays. To this end, we considered a six-layer network and set the rate of external Poisson drive to excitatory neurons in all layer networks to 6 kHz (Fig. 2a, middle column) and stimulated the first layer with pulse packets (number of spikes in each volley 50, and temporal dispersion of 2 ms) as in the two-layer motif. The initial weights of the inter-layer connections were chosen from a normal distribution with a mean of 0.2 nS and a standard deviation of 0.01 nS. In addition, transmission delays from one layer to the next were selected from a normal distribution with a mean of 30 ms and a standard deviation of 3 ms.

As shown in Figure 4a, modification of the synaptic weights between successive pairs of layers depended on the transmission delay of the corresponding connection. Specifically, connections with shorter delays were more likely to be potentiated, while those with longer delays tended to be depressed. Notably, the delay selection and stabilization of synapses in upstream layers occur more rapidly. For example, while the connections between the first and second layers were stabilized within the first 20 seconds, stabilization of the connections between the last two layers took more than 200 seconds.

Moreover, as illustrated in Figure 4b, c, the number of depressed/pruned connections was higher in the primary layers (represented in darker colors) compared to the final layers (represented in lighter colors). This progressive pruning resulted in a widening of the final distribution of delays as one advanced through the hierarchical FF network quantified by increasing std of distribution of final inter-layer delays as illustrated in Figure 4d.

To explain this observation, we note that initially a pulse packet dissipated after a few layers because of the large disparity of spike transmission delays. The wide distribution of spike transmission delays caused spikes to arrive sparsely to the subsequent layer, exerting a much weaker effect on postsynaptic neurons. Thus, it could be predicted that during pulse packet propagation in a multi-layer FF network, the signal strength from the previous layer gradually decreased. This reduction in signal strength along the network disrupted effective responses in the deeper layers. The more temporally dispersed and less strong responses of deep layers, the more disrupted the mechanism of the selection of short delays by STDP. Therefore, the evolution of the synapses between deep layers, was initially led by the baseline spiking of the neurons with no preference for the potentiation of shorter-delay connections (Figure 4a, e).

During this process, modification of the synapses between the most upstream layers led to the narrower distribution of the delays and, hence, to more synchronized inputs to the subsequent layers. Therefore, once the connections between the first layers were stabilized, modification of the connections in the next layers was accelerated and eventually inter-layer connections were evolved with the same pattern: Connections with shorter delays were more likely to survive and be potentiated. This delay-learning process took place through a forward propagation scenario as discussed above (Figure 4a, e).

Taken together, effective and fast responses were possible through the strengthening of connections with shorter transmission delays and the weakening of connections with longer transmission delays. Weakening connections with longer transmission delays reduced input dispersion, increasing the likelihood of spike generation in postsynaptic neurons. Additionally, strengthening connections with shorter transmission delays ensured faster responses from postsynaptic neurons. The significant outcome of such synaptic modifications was the network's ability to successfully propagate pulse packets (Figure 4f, lower panel) which otherwise failed to propagate across the layered network (Figure 4f, upper panel).

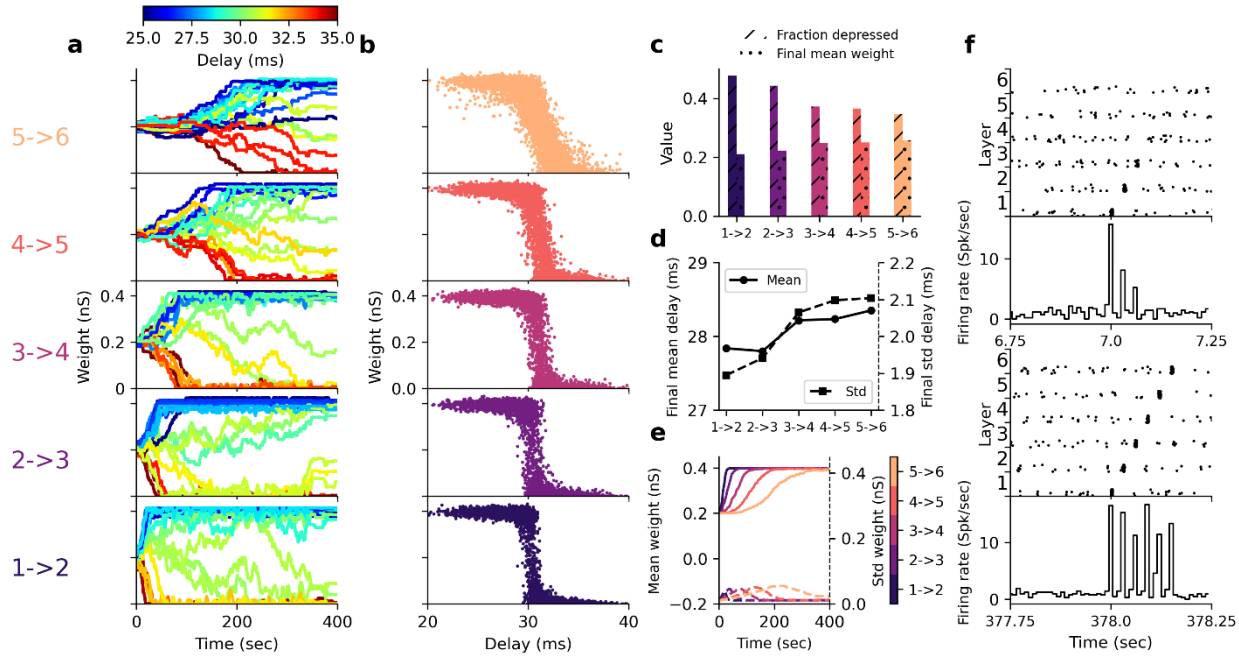

Figure 4: ***Stable propagation of a pulse packet following the elimination of connections with longer delays in a multi-layer feedforward network. (a)*** *The evolution of 20 FF connections between pairs of layers are shown. The lowest panel corresponds to the connections from layer one to layer two, and the panels are arranged sequentially up to the top panel. The colors within each panel represent the transmission delay of each connection.* ***(b)*** *The distribution of weights and delays for connections between each successive pair of layers are shown. Due to the widening of spike times through forward propagation of spike volleys, the precision of selective modification decreases as the hierarchy advances.* ***(c)*** *The number of weakened connections was higher between the initial layers.* ***(d)*** *The average transmission delay of strengthened connections was lower in the connections between the initial layers. Additionally, the standard deviation of the delays decreased due to the weakening of many connections.* ***(e)*** *The mean and standard deviation of weights in potentiated connections across all layers are shown. The faster modification of connections between the initial layers is clearly evident, reflecting more rapid adjustment of connections between initial layers.* ***(f)*** *Failed propagation before the modification of inter-layer connections (top panel), and successful propagation after the modification of inter-layer connections (bottom panel) are shown. Spiking activity of projection neurons across all layers is displayed as a scatter plot. Below the spiking activity, the output rate histogram of whole projection neurons across the six layers is shown, illustrating the improvement in synchronization and spike transmission.*

The interaction between signal transmission and delay-dependent synaptic modifications governed by spike timing-dependent plasticity created a positive feedback loop. Specifically, the preferential strengthening of synapses with shorter delays, coupled with the pruning of those with longer delays, resulted in more synchronized and robust signal propagation. This, in turn, accelerated the response of the recipient layer, further refining connectivity through additional synaptic pruning. As a consequence, the remaining connections underwent further potentiation, reinforcing this iterative process.

To investigate this effect systematically, we modulated the upper limit of synaptic weights achievable through STDP and examined its impact on network dynamics. Our results, illustrated in Figure 5a, indicate that increasing this upper limit, accelerated significantly the rate of synaptic weight modifications across layers. This enhancement was accompanied by a rise in the total number of weakened connections between successive layers of the FF network (Figure 5b). Moreover, we observed that the average overall transmission delay across all layers decreased (Figure 5c), while the mean strength of FF connections increased (Figure 5d). These structural adjustments facilitated the faster propagation of pulse packets, ultimately enhancing the

efficiency of information transfer when the upper bound of synaptic weights was elevated in the model (Figure 5e, f).

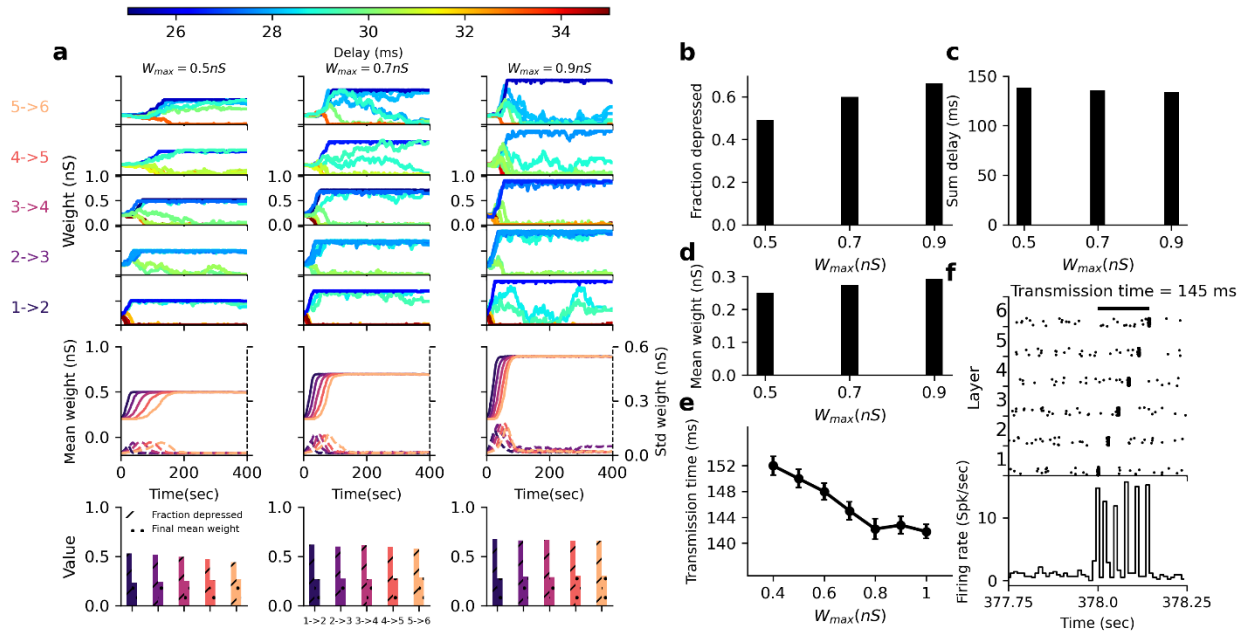

Figure 5: **Higher W_{max} enhanced rapid propagation of pulse packets. (a)** The evolution of inter-layer connections in a six-layer FF network, including the mean and standard deviation of weights for potentiated connections, as well as the number of depressed connections, is shown for three different upper limits of weights: W_{max} = 0.5 nS (left column), W_{max} = 0.7 nS (middle column), and W_{max} = 0.9 nS (right column). **(b-d)** The total number of depressed connections, sum of the mean delay of potentiated connections, and mean weights of connections after the modification for different values of W_{max}. **(e, f)** The transmission time of a single pulse packet decreased for higher values of W_{max}.

4. Discussion

Our results demonstrate that synapses with shorter transmission delays are preferentially potentiated through spike timing-dependent plasticity (STDP), leading to the progressive reduction of temporal dispersion in spike volleys. This effect enhances the synchronization of spikes arriving at downstream layers, facilitating more efficient and reliable signal propagation. The observed preference for shorter delays results from the interplay between STDP and the inherent properties of neural excitability, where postsynaptic neurons preferentially respond to earlier-arriving inputs. These findings underscore the role of temporal constraints in shaping neural computation and suggest that natural synaptic learning rules favor rapid and efficient transmission within cortical circuits.

In multi-layer FF networks, our simulations reveal a forward propagation of synaptic modification, where early layers undergo rapid reorganization, establishing conditions that subsequently accelerate plasticity in deeper layers. Initially, synaptic modifications occur without a preference for delay selection in the later layers due to the broad dispersion of spike arrival times. However, as upstream layers undergo delay-dependent plasticity, the temporal precision of transmitted spikes improves, enabling downstream layers to refine their connectivity with a

similar preference for shorter delays. This progressive stabilization of synaptic architecture indicates that hierarchical processing networks can self-organize to optimize signal propagation efficiency. Additionally, increasing the upper limit of STDP-driven synaptic weights further accelerates this process, suggesting that synaptic strength constraints play a crucial role in shaping network-wide dynamics.

Overall, our results highlight the intricate relationship between spike timing-dependent synaptic plasticity, and transmission delays in FF networks. By systematically favoring synapses with shorter delays, the network enhances both temporal fidelity and information transfer efficiency. This mechanism may have implications for understanding neural circuit organization in biological systems, where transmission delays are non-negligible and subject to plastic modifications. Furthermore, these findings may inform the design of artificial neural networks, where optimizing transmission delays could improve computational efficiency. Future research could explore how additional factors, such as inhibitory plasticity and recurrent interactions, further refine the delay-selection process and its impact on complex neural computations.

5. Conclusion

Our study revealed the existence of a self-organized mechanism that leads to faster spike timing at the postsynaptic site. Such a mechanism could involve a dynamic interaction between forward propagation of spike volleys and modification of corresponding connections through spike-timing-dependent plasticity (STDP). At the core of this interaction lies the transmission delay between populations of neurons. Transmission delay is one of the key determinant factors in timing the arrival of spikes at the postsynaptic site.

Our results showed the selective modification of connections through STDP during the repeated forward propagation of spike volleys. The mechanism underlying this selective modification relied critically on the transmission delay in forward connections: Shorter transmission delays led to potentiation, whereas longer transmission delays resulted in synaptic depression through STDP.

The boundary at which the selective mechanism begins depends critically on the spike timing of postsynaptic neurons, while the width of this boundary relies on the level of synchronization among them. Effective and rapid propagation of spike volleys enables a rapid and precise selective mechanism, which in turn facilitates more efficient and faster propagation.

References

Caporale, N., & Dan, Y. (2008). Spike timing–dependent plasticity: a Hebbian learning rule. *Annu. Rev. Neurosci, 31*(1), 25-46. https://doi.org/10.1146/annurev.neuro.31.060407.125639

Do, H. (1949). *The organization of behavior.* New York.

Esfahani, Z. G., Gollo, L. L., & Valizadeh, A. (2016). Stimulus-dependent synchronization in delayed-coupled neuronal networks. *Scientific Reports, 6*(1), 23471. https://doi.org/10.1038/srep23471

Gerstner, W., & Kistler, W. M. (2002). *Spiking neuron models: Single neurons, populations, plasticity.* Cambridge University Press. https://doi.org/10.1017/CBO9780511815706

Gewaltig, M.-O., & Diesmann, M. (2007). Nest (neural simulation tool). *Scholarpedia, 2*(4), 1430. https://doi.org/10.3389/neuro.11.012.2008

Ghasemi Esfahani, Z., & Valizadeh, A. (2014). Zero-lag synchronization despite inhomogeneities in a relay system. *PLOS ONE, 9*(12), e112688. https://doi.org/10.1371/journal.pone.0112688

Guyonneau, R., VanRullen, R., & Thorpe, S. J. (2005). Neurons tune to the earliest spikes through STDP. *Neural Computation, 17*(4), 859–879. https://doi.org/10.1152/jn.90295.2008

Kress, G. J., Dowling, M. J., Meeks, J. P., & Mennerick, S. (2008). High threshold, proximal initiation, and slow conduction velocity of action potentials in dentate granule neuron mossy fibers. *Journal of Neurophysiology, 100*(1), 281–291. https://doi.org/10.1152/jn.90295.2008

Kumar, A., Rotter, S., & Aertsen, A. (2008). Conditions for propagating synchronous spiking and asynchronous firing rates in a cortical network model. *Journal of Neuroscience, 28*(20), 5268–5280. https://doi.org/10.1523/JNEUROSCI.2542-07.2008

Kumar, A., Rotter, S., & Aertsen, A. (2010). Spiking activity propagation in neuronal networks: Reconciling different perspectives on neural coding. *Nature Reviews Neuroscience, 11*(9), 615–627. https://doi.org/10.1038/nrn2886

Kusano, K. (1966). Electrical activity and structural correlates of giant nerve fibers in Kuruma shrimp (Penaeus japonicus). *Journal of Cellular Physiology, 68*(3), 361–383. https://doi.org/10.1002/jcp.1040680315

Madadi Asl, M., Valizadeh, A., & Tass, P. A. (2018). Dendritic and axonal propagation delays may shape neuronal networks with plastic synapses. *Frontiers in Physiology, 9*, 1849. https://doi.org/10.3389/fphys.2018.01849

Madadi Asl, M., Valizadeh, A., & Tass, P. A. (2023). Decoupling of interacting neuronal populations by time-shifted stimulation. *PLOS Computational Biology, 19*(2), e1010853. https://doi.org/10.1371/journal.pcbi.1010853

Markram, H., Lübke, J., Frotscher, M., & Sakmann, B. (1997). Regulation of synaptic efficacy by coincidence of postsynaptic APs and EPSPs. *Science, 275*(5297), 213–215. https://doi.org/10.1126/science.275.5297.213

Morrison, A., Straube, S., Plesser, H. E., & & Diesmann, M. (2007). Exact subthreshold integration with continuous spike times in discrete-time neural network simulations. *Neural Computation, 19*(1), 47–79. https://doi.org/10.1162/neco.2007.19.1.47

Pariz, A., Fischer, I., Valizadeh, A., & Mirasso, C. (2021). Transmission delays and frequency detuning can regulate information flow between brain regions. *PLoS Computational Biology, 17*(4), e1008129. https://doi.org/10.1371/journal.pcbi.1008129

Pérez, T., Garcia, G. C., Eguíluz, V. M., Vicente, R., Pipa, G., & Mirasso, C. (2011). Effect of the topology and delayed interactions in neuronal networks synchronization. *PLOS ONE, 6*(5), e19900. https://doi.org/10.1371/journal.pone.0019900

Rezaei, H., Aertsen, A., Kumar, A., & Valizadeh, A. (2020). Facilitating the propagation of spiking activity in feedforward networks by including feedback. *PLoS Computational Biology, 16*(8), e1008033. https://doi.org/10.1371/journal.pcbi.1008033

Roohi, N., & Valizadeh, A. (2022). Role of interaction delays in the synchronization of inhibitory networks. *Neural Computation, 34*(6), 1425–1447. https://doi.org/10.1162/neco_a_01500

Sadeghi, S., & Valizadeh, A. (2014). Synchronization of delayed coupled neurons in presence of inhomogeneity. *Journal of Computational Neuroscience, 36*, 55–66.mailto: https://doi.org/10.1007/s10827-013-0461-9

Song, S., Miller, K. D., & Abbott, L. F. (2000). Competitive Hebbian learning through spike-timing-dependent synaptic plasticity. *Nature Neuroscience, 3*(9), 919–921. https://doi.org/10.1038/78829

Suri, R. E., & Sejnowski, T. J. (2002). Spike propagation synchronized by temporally asymmetric Hebbian learning. *Biological Cybernetics, 87*(5), 440–445. https://doi.org/10.1007/s00422-002-0355-9

VanRullen, R., & Thorpe, S. J. (2001). The time course of visual processing: From early perception to decision-making. *Journal of Cognitive Neuroscience, 13*(4), 454–464. https://doi.org/10.1162/08989290152001880

Wang, H.-P., Spencer, D., Fellous, J.-M., & Sejnowski, T. J. (2010). Synchrony of thalamocortical inputs maximizes cortical reliability. *Science, 328*(5974), 106–109. https://doi.org/10.1126/science.1183108

Ziaeemehr, A., & Valizadeh, A. (2021). Frequency-resolved functional connectivity: role of delay and the strength of connections. *Frontiers in Neural Circuits, 15*, 608655. https://doi.org/10.3389/fncir.2021.608655

Ziaeemehr, A., Zarei, M., Valizadeh, A., & Mirasso, C. R. (2020). Frequency-dependent organization of the brain's functional network through delayed interactions. *Neural Networks, 132*, 155–165. https://doi.org/10.1016/j.neunet.2020.08.003